JOURNAL OF COLLOID AND INTERFACE SCIENCE 173, 334–342 (1995)

Dynamic Surface Tension of Surfactant Solutions Studied by Peaktensiometry

TOMMY HOROZOV *,[1] AND PAUL JOOS†

*Laboratory of Thermodynamics and Physico-Chemical Hydrodynamics, Faculty of Chemistry, University of Sofia, 1 James Bouchier Ave., 1126 Sofia, Bulgaria; and †Department of Chemistry, University of Antwerp, U.I.A. Universiteitsplein 1 B-2610, Wilrijk, Belgium

Received August 3, 1994; accepted November 22, 1994

The dynamic surface tension (DST) of decanoic acid, Triton X-100, and Brij 58 solutions is studied by the so-called "peaktensiometry" method. The obtained results are interpreted by a theoretical model for diffusion-controlled adsorption. Reasonable values for diffusivities of the studied surfactants are obtained. The applicability of the peaktensiometry method to studies of the DST of submicellar and micellar surfactant solutions is demonstrated.

INTRODUCTION

There is a great variety of experimental methods for the study of the dynamic surface tension (DST) of surfactant solutions (1–5). Some of them are based on surface tension measurements during periodically (2, 3) or continuously expanded solution/air interfaces (4, 5). Very recently a new experimental method, called "peaktensiometry," was proposed by van Uffelen and Joos (6). This method is based on a measurement of the DST of a linearly expanded solution/air surface. The experiments are carried out in a Teflon trough supplied with a Teflon barrier. The barrier is moved at a constant speed, thus expanding solution/air interface. The latter has been initially in equilibrium with the bulk of the solution. The surface tension measured by a Wilhelmy plate passes through a maximum (a peak) during the surface expansion. A theoretical model for the case of diffusion-controlled adsorption has been proposed. The model allows calculation of the surfactant diffusivity from the experimental data if the equilibrium surfactant adsorption is known. The experimental results for relatively diluted solutions of decanoic acid have been in agreement with the theory. The experimental setup used in Ref. (6), however, does not allow studies of surfactant solutions for which the equilibrium surface tension is lower than ~45 dyn/cm. This makes the experimental technique inapplicable in the concentration range close to the critical micellization [illegible] (CMC), which is of main interest for the practice.

The aims of the present work are (i) further [illegible] of the theoretical model with different surfactants and (ii) an improvement of the experimental setup for the peaktensiometry technique in order to enlarge its applicability to wider concentration range.

Experiments with different kind of barriers in a wide concentration range of surfactants have been performed. The best results have been obtained with a glass barrier. In this case it has been possible to conduct experiments at any surfactant concentration, independent of the surface tension value. The results obtained for decanoic acid and the nonionic surfactants Brij 58 and Triton X-100 are in agreement with the predictions of the theory.

THEORY

The theory of the peaktensiometry method is given in detail in Ref. (6). Here we will review only the main points together with an analysis of the predictions of the theoretical model.

1. The General Case of Diffusion-Controlled Adsorption onto an Expanding Solution/Air Interface

The convective diffusion equation taken in its form approximated according to van Voorst Vader *et al.* (4) has been solved in Ref. (6) (see also Ref. (7)). It reads

$$\frac{\partial c}{\partial t} - \theta z \frac{\partial c}{\partial z} = D \frac{\partial^2 c}{\partial z^2}, \qquad [1$$

where c is the surfactant concentration, t is time, z is coordinate normal to the surface and directed towards the bulk of the solution, and D is the surfactant diffusivity. θ is a rate of surface expansion defined by the formula

$$\theta = \frac{d \ln \Omega}{dt}, \qquad [2$$

[1] To whom correspondence should be addressed.

0021-9797/95 $12.00

where Ω is the area of the surface. Equation [1] has been solved assuming small deviations from equilibrium under the following boundary and initial conditions:

$$\frac{d\Gamma}{dt} + \theta\Gamma = D\frac{\partial c}{\partial z}; \quad c(0, t) = c_s(t) \quad \text{at } z = 0 \quad [3a]$$

$$\lim_{z\to\infty} c(z, t) = c_0; \quad \lim_{z\to\infty} \frac{\partial c}{\partial z} = 0 \quad [3b]$$

$$c(z, 0) = c_0; \quad \Gamma(0) = \Gamma_e \quad \text{at } t = 0. \quad [4]$$

Here, Γ is the surfactant adsorption, c_s is the surfactant concentration in the subsurface layer, c_0 is the surfactant concentration in the bulk far from the interface, and Γ_e is the equilibrium adsorption of the surfactant. By using the approach described by Levich *et al.* (8), one obtains the final solution

$$\Delta\sigma = G\frac{f(t) - 1}{f(t)}\frac{1}{1 + \left(\frac{dc}{d\Gamma}\right)_e\sqrt{\frac{4D\tau}{\pi f^2(t)}}}, \quad [5]$$

where $f(t) = \Omega(t)/\Omega(0)$, $\tau = \int_0^t f^2(\xi)d\xi$, and $\Delta\sigma = \sigma(t) - \sigma_e$ is the deviation of the surface tension σ from its equilibrium value σ_e. $G = -d\sigma/d \ln \Gamma$ is the Gibbs elasticity and subscript "e" denotes an equilibrium value. In such a form, Eq. [5] is applicable to any law of surface expansion under the following two requirements:

(i) small deviations from equilibrium, and
(ii) a known law of surface expansion, i.e., $\Omega = \Omega(t)$.

2. *The Case of a Linearly Expanded Surface: Peaktensiometry*

Following the approach of van Uffelen and Joos (6), the law of surface expansion in this case reads

$$\Omega(t) = \Omega(0)(1 + \alpha t), \quad [6]$$

where $\alpha = (1/\Omega(0))(d\Omega(t)/dt)$ is a parameter since $d\Omega(t)/dt$ = const. The physical meaning of α becomes more clear if we rewrite Eq. [6] in terms of the rate of surface expansion, θ:

$$\theta(t) = \frac{\alpha}{1 + \alpha t}. \quad [7]$$

It is seen that at time equal to zero, $\theta(0) = \alpha$. Hence, α is the initial rate of surface expansion. It is obvious from Eq. [7] that for a linearly expanded surface the rate of surface expansion is not constant. It decreases with time, which is illustrated in Fig. 1. There $\theta(t)$ is scaled by its initial value, i.e., by α, and its trend with time for two different values of α is compared with the case θ = const. One can see that the higher initial rate of surface expansion, α, leads to the faster decrease of the expansion rate, θ. The latter tends to zero at infinite time. For this particular case of surface expansion Eq. [5] yields

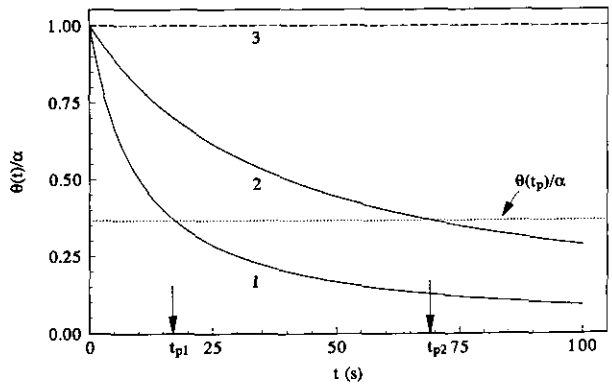

FIG. 1. Relative rate of surface expansion $\theta(t)$ versus time in the case of a linearly expanded surface at different α (in s^{-1}): 0.1 (curve 1) and 0.025 (curve 2). The dashed line (3) represents the case of constant expansion rate $\alpha = \theta$ = const.

$$\Delta\sigma = G\theta t \Big/ \left(1 + \sqrt{\frac{4t}{3\pi t_D}}\sqrt{\frac{\alpha^2t^2 + 3\alpha t + 3}{\alpha^2t^2 + 2\alpha t + 1}}\right), \quad [8]$$

where $t_D = (1/D)/(d\Gamma/dc)_e^2$ is a characteristic diffusion time. For not very small times, when $t \gg t_D$, the unity in the denominator of Eq. [8] can be omitted. In this case, after simple mathematical calculations, Eq. [8] transforms into

$$\Delta\sigma = \frac{RT\Gamma_e^2}{c_0}\sqrt{\frac{3\pi\alpha}{4D}}\sqrt{\frac{\alpha t}{\alpha^2t^2 + 3\alpha t + 3}}. \quad [9]$$

Equation [9] predicts a maximum (a peak) in the $\Delta\sigma$ versus time curve at time $t = t_p$, which is given by the formula

$$t_p = \frac{\sqrt{3}}{\alpha}. \quad [10]$$

The substitution of Eq. [10] in Eq. [7] yields the expression

$$\theta(t_p) = \frac{\alpha}{1 + \sqrt{3}},$$

which suggests that at the moment of the peak the rate of surface expansion is approximately equal to 37% of its initial value, α. t_p does not depend on the surfactant concentration

or the type of surfactant. The same is valid for the rate of surface expansion at the moment of the peak. The curves 1 and 2 in Fig. 1 show that at times longer than t_p the rate of surface expansion decreases more slowly when the initial rate of expansion, α, is smaller. This suggests that at smaller α the peak in the $\Delta\sigma$ versus time curve will appear later and will be flatter in comparison with the case of greater α. The height of the peak, however, will depend on the surfactant concentration and the properties of the surfactant. This conclusion follows from the equation

$$\Delta\sigma_p = \beta \frac{RT\Gamma_e^2}{c_0\sqrt{D}}\sqrt{\alpha} \qquad [11]$$

obtained from Eq. [9] at $t = t_p$. Here $\Delta\sigma_p = \Delta\sigma(t_p)$ and β is a numerical constant given by the expression

$$\beta = \sqrt{\frac{\pi\sqrt{3}}{4(2+\sqrt{3})}} \cong 0.604.$$

Eq. [11] suggests that $\Delta\sigma_p$ plotted versus $\sqrt{\alpha}$ should give a straight line with the slope

$$B = \beta \frac{RT\Gamma_e^2}{c_0\sqrt{D}} \qquad [12]$$

and the intercept $B_0 = 0$. Since the slope, B, can be obtained experimentally, it is possible to calculate the surfactant diffusivity, D, if the equilibrium adsorption, Γ_e, is known, and vice versa. The proper calculation of D, however, requires that Γ_e be known with a high precision.

The predictions of the theory in its simplified form (see Eq. [9]) can be summarized as follows: (i) $\Delta\sigma$ should pass through a maximum (a peak) within a certain time, $t = t_p$. (ii) The position of the peak in time, i.e., t_p, should not depend on any properties of the surfactant, but only on the initial rate of surface expansion, α. (iii) Under a given surfactant concentration the peak should be higher and sharper at greater α, while at smaller α it should be lower and more flat. (iv) The height of the peak, $\Delta\sigma_p$, plotted versus $\sqrt{\alpha}$ should give a straight line with a slope proportional to $\Gamma_e^2/c_0\sqrt{D}$ and an intercept equal to zero. (v) The dimensionless jump $\Delta\sigma/\Delta\sigma_p$ plotted versus the dimensionless time, t/t_p should give only one curve for all kind of surfactants, concentrations, and rates of surface expansions according to the expression

$$\frac{\Delta\sigma}{\Delta\sigma_p} = \sqrt{\frac{(2+\sqrt{3})t/t_p}{(t/t_p)^2 + \sqrt{3}t/t_p + 1}}, \qquad [13]$$

which follows from Eqs. [9], [10], and [11].

EXPERIMENT

Materials

Experiments were carried out with solutions of different surfactants in a wide concentration range. The surfactants used in this study were the following:

(a) Decanoic acid purchased from Aldrich with 99+% purity. The water solutions of this surfactant also contained 0.01 *M* HCl and 0.09 *M* NaCl. Hence, the pH was approximately 2 and the ionic strength was ~0.1 *M*. Under such conditions the dissociation of the decanoic acid is suppressed. It exists in an acid form and behaves regularly with respect to the surface properties (9).

(b) Polyoxyethylene-10-octylphenol ether, known by the commercial name Triton X-100. This nonionic surfactant, a product of Serva, has an average of 10 ethoxy groups per molecule and a molecular weight ca. 647.

(c) Polyoxyethylene-20-cetyl ether, known as Brij 58, is a product of Serva. Its molecular weight is ca. 1050 and it contains an average of 20 ethoxy groups incorporated in its molecule.

It should be mentioned that Triton X-100 and Brij 58 are in fact mixtures. However, no minimum has been observed in the equilibrium surface tension versus concentration curves at CMC (10, 11, 14), indicating that highly surface active minor components are absent. Brij 58 has been previously used for studying the adsorption kinetics and no effect due to impurities has been found (15). The recent study by Nagarajan and Wasan (16) with the same surfactant did not show any peculiarities of its surface properties. That is why we believe that both Triton X-100 and Brij 58 can be treated as pure compounds with respect to their surface properties.

Deionized water obtained with a Millipore unit was used for preparation of the surfactant solutions.

Experimental Setup

The sketch of the experimental setup is shown in Fig. 2a and 2b. A Teflon trough with length 48.1 cm, width 8.1 ± 0.1 cm, and depth ca. 0.6 cm is filled with a surfactant solution. A barrier rests on the upper side of the trough and divides the solution/air surface into two separate parts. The barrier can be moved at a constant speed along the whole length of the trough. For this purpose a fork attached to a nut screwed onto a screw bar is used. The screw bar is turned by an electromotor supplied with a reductor. A stainless steel string (0.2 mm in diameter) is stretched along the whole length of the trough. One end of the string is tightly fixed, while the other end is attached to a stretching mechanism. The string passes above the upper side of the barrier and around three wheels mounted close to the farthermost ends of the trough. Both ends of the string are situated below the

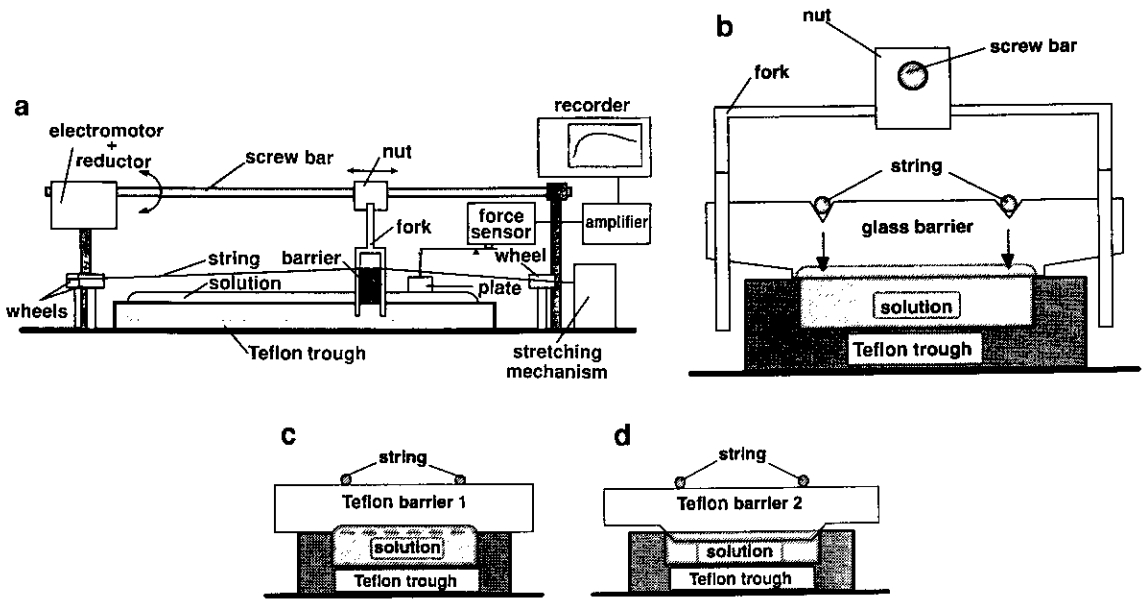

FIG. 2. Sketch of the experimental setup (a) and its cross sections with different barriers (b–d).

level of the tip of the barrier. In this way the string is banded in a vertical direction and presses the barrier down toward the trough. The use of only one string provides an equal pressure on both ends of the barrier. In this way the vertical vibrations of the barrier during its movement are damped; thus barrier velocities up to 0.9 cm/s can be achieved. This allows experiments at the high expansion rates needed to provide a detectable peak when concentrated surfactant solutions are studied. The surface tension of the solution is measured close to the one end of the trough by a platinum Wilhelmy plate. The plate hangs on the longer arm of the lever of a force sensor (gold cell, Statham, U.S.A.). The electrical signal of the sensor is amplified and recorded by a strip chart recorder (Kipp & Zonen, Holland). A similar experimental setup has been used in Ref. (6) where a rectangular Teflon barrier (a parallelepiped) has been employed (Teflon barrier 1 in Fig. 2c). A disadvantage of such a barrier is that it requires the surfactant solution to be elevated above the upper edge of the trough. This leads to leakage of the solution outside the trough when its surface tension is lower than ~45 dyn/cm. Hence a rectangular Teflon barrier is applicable only in relatively dilute solutions well below CMC. In order to perform experiments at high surfactant concentrations, we have tested two other types of barriers. The first one was a Teflon barrier with a special profile, shown in Fig. 2d (Teflon barrier 2). The second one was a glass barrier with a profile similar to that of Teflon barrier 2 (Fig. 2b). In contrast to the former, it lies above the edge of the trough, overlapping the trough wall by about 1 mm. Two small channels on the upper side of the glass barrier serve to fix it in a horizontal direction and keep the barrier attached to the trough walls during its movement. The possibility of leakage of the solution with the new barriers is avoided because the level of the solution does not exceed the edges of the trough. Teflon barrier 2 is immersed in the solution, thus separating the solution surface. The same result is achieved in the case of a glass barrier because the solution is elevated on both sides of the barrier due to the wettability of the glass.

Experimental Procedure

The experiments were carried out according to the following procedure. The trough was filled with a surfactant solution. The barrier was positioned close to the end of the trough where the surface tension was measured. After a sufficiently long time (1–3 h, depending on the surfactant and its concentration) the surface tension had practically reached its equilibrium value. Then the electromotor was turned on and the expansion of the solution/air surface was started. The change in the surface tension with time (a peaktensiogram) was recorded by the strip chart recorder. After certain time, depending on the surfactant concentration and the speed of the barrier, the motor was turned off. Then the initial rate of surface expansion, α, was calculated by the formula

$$\alpha = \frac{V}{x(0)},$$

where V is the velocity of the barrier calculated after each experiment and $x(0)$ is the initial distance between the barrier and the edge of the trough. In all experiments $x(0)$ was typi-

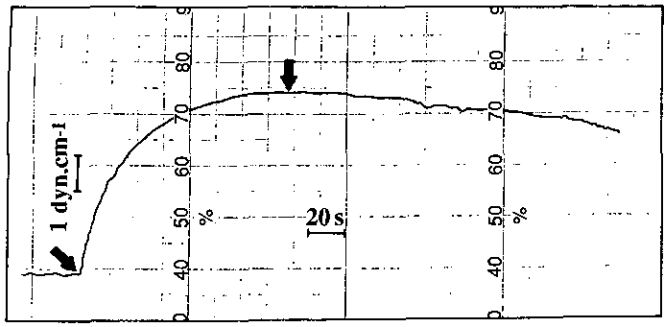

FIG. 3. A typical peaktensiogram as it has been recorded by the recorder. The beginning of surface expansion and the peak are indicated by arrows.

cally in the range 6–8 cm. The velocity of the barrier was varied either by switching the reductor stepwise or by gradually changing the power supply voltage of the electromotor.

RESULTS AND DISCUSSION

A typical peaktensiogram as recorded by the strip chart recorder is shown in Fig. 3. It is seen that the surface tension quickly increases at the beginning of surface expansion; then its increase becomes slower. At a certain moment the surface tension passes through a maximum and after that it slowly decreases. Such a trend of the surface tension during the surface expansion is in perfect qualitative agreement with the theoretical predictions. The quantitative comparison between the theory and the experimental results is given below.

1. Experiments at Concentrations below CMC

The peaktensiograms (i.e., $\Delta\sigma$ versus time curves) can be described by Eq. [9] if $\Gamma_e^2/\sqrt{D}$ is known. This quantity can be obtained from the slope of $\Delta\sigma_p$ versus $\sqrt{\alpha}$ dependence (see Eqs. [11] and [12]). The data for three surfactant solutions, 7×10^{-8} mol/cm^3 decanoic acid, 5×10^{-9} mol/cm^3 Triton X-100, and 2.5×10^{-9} mol/cm^3 Brij 58, are plotted in Fig. 4. One can see that the experimental points obtained for all three solutions lay well on their own straight lines. The height of the peak increases with increased α, which is in agreement with the theory. In the same figure data for Triton X-100 obtained by all three barriers are shown. The experimental data obtained with a glass barrier practically coincide with those obtained with Teflon barrier 1. The data obtained with Teflon barrier 2 are a little shifted. The same effect has been observed with solutions of Brij 58 above CMC (see Fig. 10, line 3). This may be due to the different hydrodynamic conditions during surface expansion when Teflon barrier 2 has been used. The parameters of the best fits are summarized in Table 1. The intercepts, B_0, of the lines are equal to zero in the range of experimental error, while the slopes B are different for different surfactants. The same result is predicted by the theoretical model. All fits are good, which follows from their small standard deviations. The relative error of the slope does not exceed 9%. The comparison between the results obtained with different barriers shows that the best are those obtained with a glass barrier. The slopes, B, are identical in the range of experimental error. Hence, the new barriers give practically the same (or even better) results as Teflon barrier 1 at low surfactant concentrations. Such a comparison is impossible at high concentrations, where Teflon barrier 1 is inapplicable. The values of B were used for calculation of the quantity $\Gamma_e^2/\sqrt{D}$ in Eq. [9]. Then the $\Delta\sigma$ versus time dependencies were calculated and compared with the measured peaktensiograms. The result is shown in Fig. 5. To make the plots clearer we have not plotted all measured data, but only those obtained at high, intermediate, and low initial rates of surface expansion, α. As predicted by the theory, the peaks are higher and sharper at high α, while at low α they are lower and flatter. The theory describes better the data obtained at intermediate and low initial rates of surface expansion, in which cases the peak is not very large. The discrepancies between the theory and the experimental data are greater at high α. This could be expected bearing in mind that small deviations from equilibrium have been assumed in the theoretical model. The general agreement between theory and experiment even at high initial expansion rates (see also Fig. 9) suggests that in practice the requirement for small deviations from equilibrium is not so strict. This is supported also by other studies. For instance, desorption from spread monolayers of lauric acid has been studied in Ref. (17), and even at large deviations from equilibrium ($\Delta\sigma \sim 20$ dyn/cm) the experimental results have been successfully described by a linear theory. Anyhow, it is expected that at large $\Delta\sigma$ the present theory describes the results semiquantitatively.

The measured time of the peak, t_p, is plotted versus

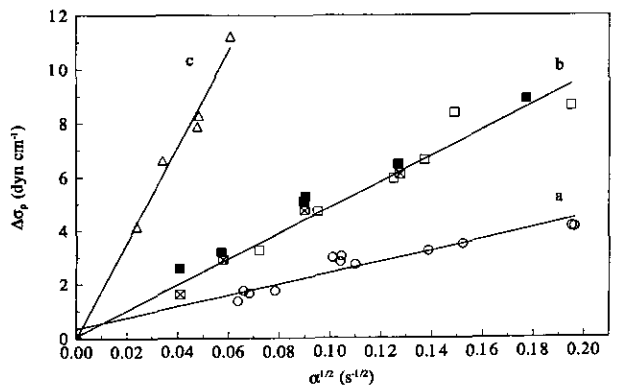

FIG. 4. Height of the peak $\Delta\sigma_p$ versus $\sqrt{\alpha}$ in the cases of decanoic acid (a); Triton X-100 (b) obtained with a glass barrier (⊠), Teflon barrier 1 (□), and Teflon barrier 2 (■); and Brij 58 (c). The lines are the best linear fits. The other details are given in Table 1.

TABLE 1
Parameters of the Best Linear Fits Obtained from the Data in Fig. 4

Surfactant	$c_0 \times 10^8$ (mol cm^{-3})	Barrier	B_0 (dyn cm^{-1})	B (dyn cm^{-1} s$^{1/2}$)	Standard deviation (dyn cm^{-1})
Decanoic acid	7.0	Teflon 1	0.3 ± 0.2	20.76 ± 1.68	0.32
Triton X-100	0.5	Teflon 1	0.1 ± 0.5	47.76 ± 4.25	0.65
		Teflon 2	0.4 ± 0.3	48.06 ± 2.81	0.42
		Glass	−0.1 ± 0.2	50.02 ± 3.11	0.30
Brij 58	0.25	Teflon 1	0.0 ± 0.4	178.55 ± 9.82	0.48

$1/\alpha$ in Fig. 6. According to Eq. [10], the data should lie on a straight line with slope $\sqrt{3}$. One can see that the experimental results are in agreement with this prediction. The deviations are greater at small initial rates of surface expansion. It should be noted, however, that at small α the peak is very flat and its exact position in time cannot be determined very precisely (see Fig. 5, curve 3).

The effect of surfactant concentration is seen in Fig. 7, where data for Brij 58 are plotted. It is seen that the slope of the lines decreases with an increase in the surfactant concentration. This fact, together with Eq. [11], suggests that in the studied concentration region the equilibrium adsorption, Γ_e, changes only slightly; hence the quantity Γ_e^2/c_0 decreases with an increase of concentration, c_0. This conclusion is supported by the plots in Fig. 8, where the slope, B, is plotted together with $(\Gamma_e/\Gamma_\infty)^2$ versus surfactant concentration. Γ_e has been calculated

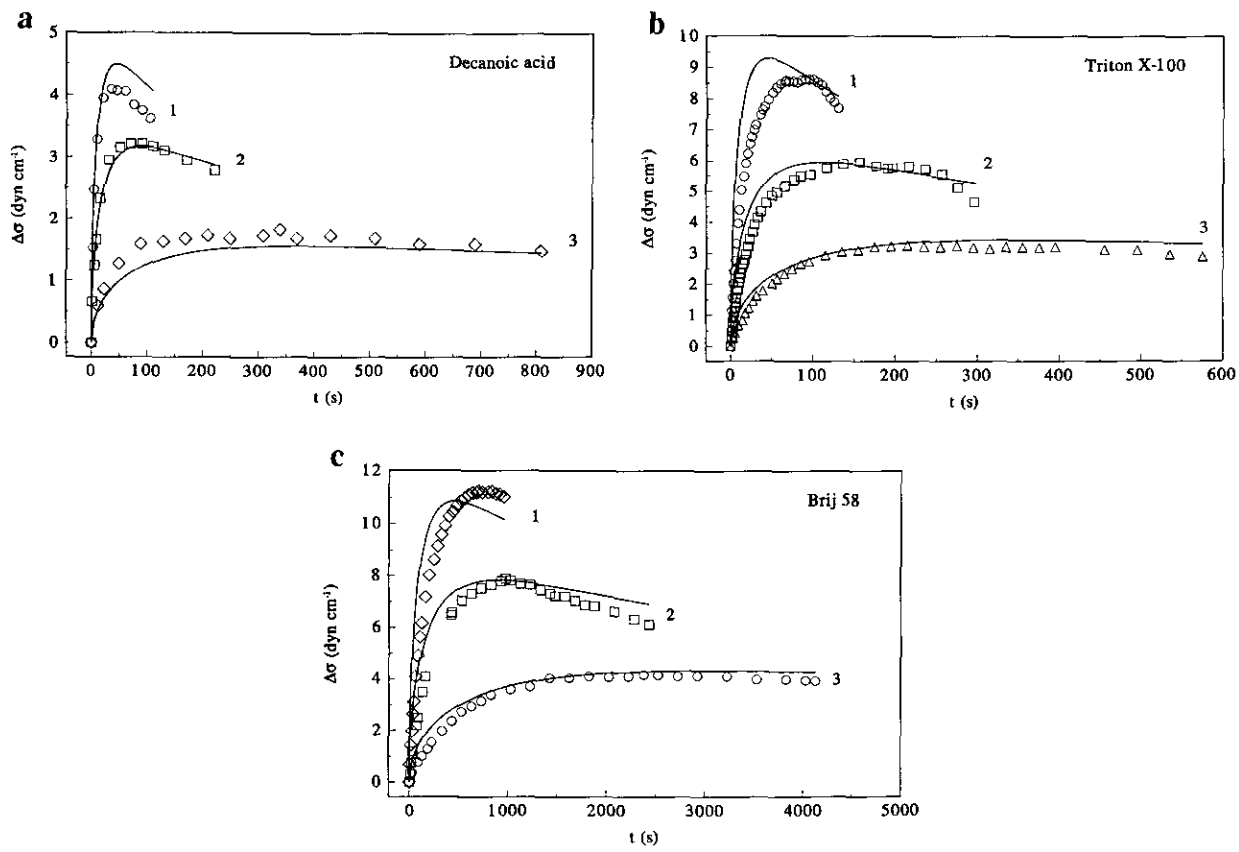

FIG. 5. Typical peaktensiograms obtained in solutions of: (a) 7×10^{-8} mol/cm^3 decanoic acid at α ($\times 10^3$ s^{-1}) equal to 38 (curve 1), 19 (curve 2), and 4.6 (curve 3); (b) 5×10^{-9} mol/cm^3 Triton X-100 at α ($\times 10^3$ s^{-1}) equal to 38 (curve 1), 16 (curve 2), and 5.2 (curve 3); and (c) 2.5×10^{-9} mol/cm^3 Brij 58 at α ($\times 10^3$ s^{-1}) equal to 3.7 (curve 1), 1.9 (curve 2), and 0.6 (curve 3). The lines are drawn according to Eq. [9].

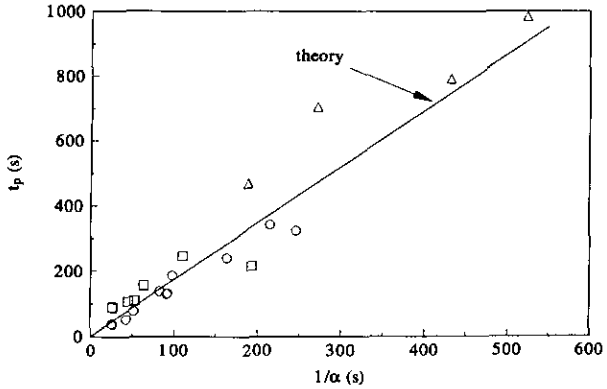

FIG. 6. Time of the peak t_p versus $1/\alpha$ obtained in solutions of 7×10^{-8} mol/cm^3 decanoic acid (○), 5×10^{-9} mol/cm^3 Triton X-100 (□), and 2.5×10^{-9} mol/cm^3 Brij 58 (△).

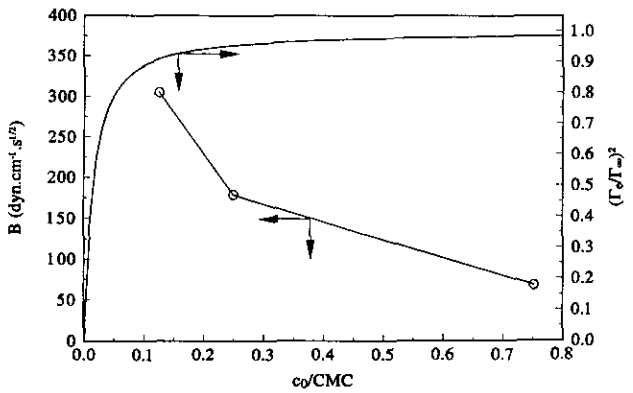

FIG. 8. Slope of the lines B, from Fig. 7, and Γ_e^2 versus Brij 58 concentration. Γ_e has been calculated by the Langmuir isotherm (10). CMC = 1×10^{-8} mol/cm^3.

by the Langmuir isotherm, which is operative for Brij 58 (10).

In Fig. 9 is plotted the dimensionless jump $\Delta\sigma/\Delta\sigma_p$ versus dimensionless time, t/t_p, measured in submicellar solutions of decanoic acid, Triton X-100, and Brij 58 under high and low initial rates of surface expansion, α. The line is drawn according to Eq. [13]. One can see that the experimental data obtained for different surfactants under different concentrations and initial expansion rates do not deviate to a large extent from the theoretical curve, but follow the general trend predicted by the theory.

2. *Experiments at Surfactant Concentrations above CMC*

In order to verify the applicability of the new barriers at high surfactant concentrations, some experiments above CMC have been performed. The height of the peak, $\Delta\sigma_p$, obtained for Brij 58 and Triton X-100 is plotted versus $\sqrt{\alpha}$ in Fig. 10. Surprisingly, the experimental data at concentrations higher than CMC lie on straight lines, as at concentrations below CMC. These data can be described by the present theory if we accept that a local equilibrium between the monomers and the micelles is established in the bulk of the solution. This seems plausible since the time scale of the experiments (on the order of hundreds of seconds) is much greater than the timescale of micellar disintegration (less than several seconds (12, 18)). Under this assumption the relation between the dynamic surface tension and time remains the same as for a purely diffusion controlled process if the diffusivity of monomers, D, is replaced by an effective (or apparent) diffusion coefficient, D_{eff} (19, 20). In this way Eq. [11] can be rewritten as

$$\Delta\sigma_p = \beta \frac{RT\Gamma_{CMC}^2}{CMC\sqrt{D_{eff}}}\sqrt{\alpha}, \qquad [14]$$

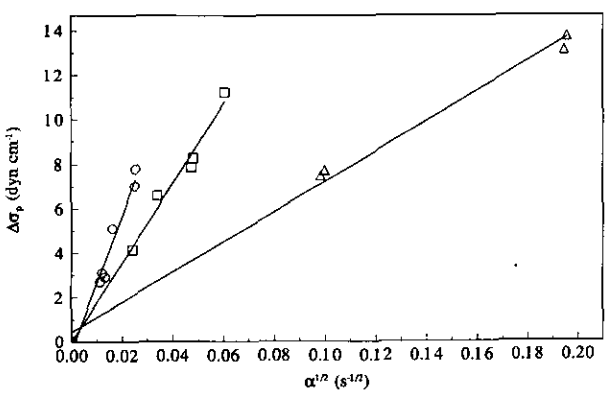

FIG. 7. Height of the peak versus $\sqrt{\alpha}$ obtained in Brij 58 solutions at concentrations equal to 1.25×10^{-9} mol/cm^3 (○), 2.5×10^{-9} mol/cm^3 (□), and 7.52×10^{-9} mol/cm^3 (△).

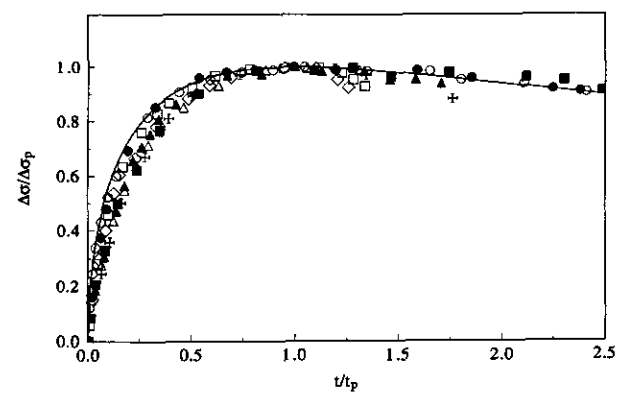

FIG. 9. Dimensionless jump $\Delta\sigma/\Delta\sigma_p$ versus dimensionless time measured in submicellar solutions of: 7×10^{-8} mol/cm^3 decanoic acid (○, ●), 5×10^{-9} mol/cm^3 Triton X-100 (□, ■), and Brij 58 at concentrations 1.25×10^{-9} mol/cm^3 (+), 2.5×10^{-9} mol/cm^3 (△, ▲), and 7.52×10^{-9} mol/cm^3 (◇) under high (empty figures) and low (full figures) initial rates of surface expansion, α. The line is drawn according to Eq. [13].

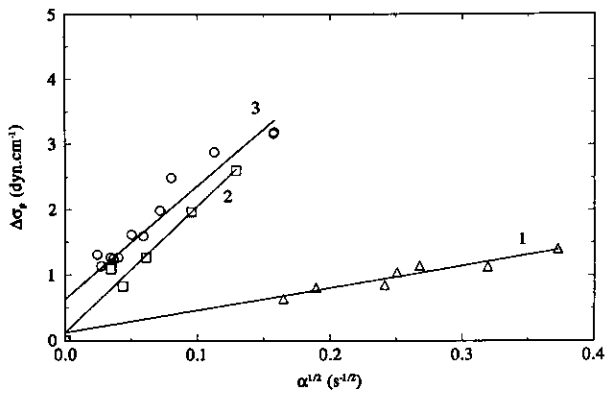

FIG. 10. Height of the peak versus $\sqrt{\alpha}$ obtained in micellar solutions of 3.1×10^{-7} mol/cm^3 Triton X-100 (curve 1), 2×10^{-8} mol/cm^3 Brij 58 (curve 2), and 3×10^{-8} mol/cm^3 Brij 58 (curve 3). The lines are drawn according to Eq. [14].

where Γ_{CMC} is the equilibrium adsorption at CMC. In Ref. (19) an expression for the effective diffusivity has been obtained,

$$D_{eff} = D\left(1 + \frac{c_0 - \text{CMC}}{\text{CMC}}\right) \times \left(1 + \frac{c_0 - \text{CMC}}{\text{CMC}} \frac{D_m}{D}\right), \quad [15]$$

where c_0 is the total surfactant concentration and D_m is the diffusivity of the micelles. It is obvious from Eq. [15] that D_{eff} can be much greater than the diffusivity of the monomers, D, and should increase with the increase of surfactant concentration. Hence, the lower slope of curve 3 in Fig. 10 can be related to the higher D_{eff} compared to that at the lower concentration (curve 2).

The properties of all studied surfactant solutions are summarized in Table 2. The values of the equilibrium adsorption Γ_e have been calculated as follows: (a) For decanoic acid it was calculated by the Frumkin isotherm,

$$c_0 = \frac{a\Gamma_e}{\Gamma_\infty - \Gamma_e} \exp\left[H\left(1 - 2\frac{\Gamma_e}{\Gamma_\infty}\right)\right],$$

with a saturation adsorption $\Gamma_\infty = 5.3 \times 10^{-10}$ mol/cm^2, an interaction parameter $H = 1.8$, and a Langmuir–von Szyskowski constant $a = 1.26 \times 10^{-8}$ mol/cm^3 (9). (b) For Triton X-100 it was calculated by the Temkin isotherm,

$$\sigma_e = \sigma_w - b\Gamma_e^2,$$

where $\sigma_w = 72.28$ dyn/cm is the surface tension of pure water at 23°C (13) and $b = 3.67 \times 10^{20}$ dyn cm^3/mol^2 is a constant taken from Ref. (14). (c) For Brij 58 it was calculated by the Langmuir isotherm,

$$\Gamma_e = \Gamma_\infty \frac{c_0}{a + c_0},$$

with $\Gamma_\infty = 2.7 \times 10^{-10}$ mol/cm^2 and $a = 6.2 \times 10^{-11}$ mol/cm^3 (10). Then the diffusivities D and D_{eff} were calculated using Eq. [12] and Eq. [14], respectively. The values of D obtained for Brij 58 solutions practically coincide with the expected value, 5×10^{-6} cm^2/s. The value obtained for decanoic acid seems a bit high but still reasonable, while D calculated for Triton X-100 is approximately twice as high. The application of the Langmuir isotherm, which is also operative for Triton X-100 (14), gives much a greater value of D, equal to $\sim 20 \times 10^{-6}$ cm^2/s. Hence, the value of the diffusivity is very sensitive to the value of the equilibrium adsorption used for its calculation. This can be expected bearing in mind that in such calculations Γ_e is of the fourth power (see Eq. [12]). Hence, for the proper calculation of D, the equilibrium adsorption of the surfactant, Γ_e, should

TABLE 2
Properties of Surfactant Solutions Obtained at 23 ± 1°C

Surfactant	$c_0 \times 10^8$ (mol cm^{-3})	c_0/CMC	$D \times 10^6$ (cm^2 s^{-1})	$D_{eff} \times 10^6$ (cm^2 s^{-1})	$\Gamma_e \times 10^{10}$ (mol cm^{-2})	σ_e (dyn cm^{-1})
Decanoic acid	7.0	0.7	7.1 ± 1.1		5.11	50.9
Triton X-100	0.5	0.032	9.9 ± 1.2[a]		2.26	54.1
	31.0	2		9.1 ± 2.6	3.28	29.6
Brij 58	0.125	0.125	6.6 ± 1.1		2.57	52.2
	0.250	0.25	5.3 ± 0.6		2.63	47.7
	0.752	0.752	4.4 ± 0.4		2.678	41.3
	2.0	2		30.5 ± 5.5	2.683	41.2
	3.0	3		38.1 ± 6.2	2.683	41.2

[a] An average value obtained with teflon barrier I and a glass barrier.

be exactly known. As it has been expected, the effective diffusivity, D_{eff}, is higher for the more concentrated micellar solution of Brij 58 and much higher than the diffusivity of monomers, D. In order to compare the experimental values of D_{eff} with those predicted by Eq. [15] one can accept $D_m/D = 0.25$ (see Refs. 10, 19, and 20), $D = 5.4 \times 10^{-6}$ cm^2/s for Brij 58 (a mean value obtained below CMC), and $D = 5 \times 10^{-6}$ cm^2/s for Triton X-100 (instead of the value 9.9×10^{-6} cm^2/s, which seems too high). The calculated values of D_{eff} are 13.5×10^{-6} cm^2/s (2×10^{-8} mol/cm^3 Brij 58), 24.3×10^{-6} cm^2/s (3×10^{-8} mol/cm^3 Brij 58), and 12.5×10^{-6} cm^2/s (3.1×10^{-7} mol/cm^3 Triton X-100). The quantitative agreement between the theory and the experiments with micellar solutions is quite satisfactory. This encouraging result suggests that the peaktensiometry method can be applied even at concentrations above CMC. However, more profound studies in this concentration range are needed.

CONCLUSIONS

The experimental results obtained by the peaktensiometry method for solutions of decanoic acid, Triton X-100, and Brij 58 are in agreement with the predictions of the theoretical model. The values of the surfactant diffusivities, $\approx 5 \times 10^{-6}$ cm^2/s (Brij 58), 7×10^{-6} cm^2/s (decanoic acid), and 10×10^{-6} cm^2/s (Triton X-100), calculated from the experimental data below CMC are reasonable. The equilibrium adsorption of the surfactant, Γ_e, should be exactly known for the proper calculation of the diffusivity.

The improved experimental setup allows studies in a wide range of surfactant concentrations—from well below CMC up to several times higher than CMC. The best results are obtained with a glass barrier. In this case experiments can be made at any surfactant concentration, independent of the surface tension value.

The peaktensiometry method can be successfully used for studies of the dynamic surface tension of submicellar and, possibly, of micellar solutions of not very "fast" surfactants such as Brij 58 and Triton X-100.

REFERENCES

1. Defay, R., and Petre, G., *in* "Surface and Colloid Science" (E. Matijevic, Ed.). Wiley, New York, 1971.
2. Lucassen, J., and van den Tempel, M., *J. Colloid Interface Sci.* **41,** 491 (1972).
3. Lunkenheimer, K., Hartenstein, C., Miller, R., and Wantke, K. D., *Colloids Surf.* **8,** 271 (1984).
4. van Voorst Vader, F., Erkens, Th. F., and van den Tempel, M., *Trans. Faraday Soc.* **60,** 1170 (1964).
5. MacLeod, C. A., and Radke, C. J., *J. Colloid Interface Sci.* **160,** 435 (1993).
6. van Uffelen, M., and Joos, P., *Colloids Surf. A* **85,** 119 (1994).
7. Joos, P., and van Uffelen, M., *J. Colloid Interface Sci.* **155,** 271 (1993).
8. Levich, V. G., Khaikin, B. I., and Belokonos, E. D., *Elektrochimija* **1,** 1273 (1965).
9. Marcipont, Ch., Thesis, Univ. of Antwerp, Antwerp, 1979.
10. van Hunsel, J., Ph.D. thesis, Univ. of Antwerp, Antwerp, 1987.
11. Rillaerts, E., Ph.D. thesis, Univ. of Antwerp, Antwerp, 1981.
12. Horozov, T. S., Dushkin, C. D., "Proc. First World Congress on Emulsion," Paris 19–22, October, 1993.
13. "Handbook of Chemistry and Physics" (R. C. Weast, Ed.), 55th ed., p. F-43. CRC Press, Boca Raton, FL 1974.
14. Fang, J., Ph.D. thesis, Ch. VIII, Univ. of Antwerp, Antwerp, 1993.
15. van Hunsel, J., and Joos, P., *Colloid Polym. Sci.* **267,** 1026 (1989).
16. Nagarajan, R., and Wasan, D. T., *J. Colloid Interface Sci.* **159,** 164 (1993).
17. Joos, P., and Bleys, G., *Colloid Polym. Sci.* **261,** 1038 (1983).
18. Aniansson, E. A. G., Wall, S. N., Almgren, M., Hoffman, H., Kielmann, I., Ulbricht, W., Zana, R., Lang, J., Tondre, C., *J. Phys. Chem.* **80,** 905 (1976).
19. Joos, P., and van Hunsel, J., *Colloids Surf.* **33,** 99 (1988).
20. Lucassen, J., *Faraday Disc. Chem. Soc.* **55,** 76 (1975).